$K^\pi=0^+$ band moment of inertia anomaly

J. Y. Zeng, C. S. Wu, L. Cheng, and C. Z. Lin
Department of Physics, Peking University, Beijing, China
and China Center of Advanced Science and Technology (World Laboratory), Center of Theoretical Physics, Beijing, China
(Received 28 September 1989)

The moments of inertia of $K^\pi=0^+$ bands in the well-deformed nuclei are calculated by a particle-number-conserving treatment for the cranked shell model. The very accurate solutions to the low-lying $K^\pi=0^+$ bands are obtained by making use of an effective K truncation. Calculations show that the main contribution to the moments of inertia comes from the nucleons in the intruding high-j orbits. Considering the fact that no free parameter is involved in the calculation and no extra inert core contribution is added, the agreement between the calculated and the observed moments of inertia of 0^+ bands in ^{168}Er is very satisfactory.

I. INTRODUCTION

Commonly, the lowest excited $K^\pi=0^+$ band of a well-deformed nucleus is known as the β-vibrational band.[1] From the analysis of the experimental results it has been noted that the moment of inertia of the lowest excited $K^\pi=0^+$ band quite often differs from those of the ground band and the γ-vibrational band. This problem was first raised by Bohr and Mottelson[2] and the inability of the standard (sd) interaction boson model (IBM) to account for this deviation has been stressed by Casten and Warner.[3] Recently, by using a $1/N$ expansion technique (N being the number of bosons), Kuyucak and Morrison[4] showed that the IBM with arbitrary kinds of bosons (i.e., allowing for arbitrary high-spin bosons) and interactions leads to the same moment of inertia for all bands, and hence does not allow such a deviation to leading order.

However, it has been noted that there are usually several low-lying excited $K^\pi=0^+$ bands, not all of which can be accommodated in the collective model space. The well-known examples are the four low-lying $K^\pi=0^+$ bands that are well established in ^{168}Er.[5,6] A remarkable feature of the $K^\pi=0_2^+$ band (bandhead at 1217 keV) and 0_4^+ band (bandhead at 1833 keV) is that their moments of inertia are almost equal ($2\mathcal{I}/\hbar^2\sim 100$ MeV^{-1}), but much larger than those of the ground band ($2\mathcal{I}_0/\hbar^2\sim 75.2$ MeV) and the γ-vibrational band (bandhead at 821 keV, $2\mathcal{I}_\gamma/\hbar^2\sim 80.7$ MeV^{-1}). The moment of inertia of the $K^\pi=0_3^+$ band (bandhead at 1422 keV), $2\mathcal{I}/\hbar^2\sim 84.7$ MeV) is also larger than that of the ground band. These excited $K^\pi=0^+$ bands are connected to the ground band by $B(E2)$ values that are a fraction of the single-particle (Weisskopf) unit B_w, and therefore cannot be interpreted as β vibration.[2,7] The absence of low-lying β vibration in this mass region is expected from the Nilsson single-particle level scheme.[1,2] It was also pointed out[4] that the $K^\pi=0^+$ rotational bands with markedly different moments of inertia are outside of the IBM model space. It has been suggested[8] that these excited $K^\pi=0^+$ bands may be regarded as two-quasiparticle states or certain superpositions of them.

The cranked shell model (CSM), originally introduced by Inglis,[9] and its generalization provided a basis for interpreting the moments of inertia observed in the rotational bands at low angular momenta.[10–12] By considering an uniform rotation around the x axis with cranking frequency ω, the CSM Hamiltonian is written as

$$H_{\rm CSM}=H_{\rm intr}-\hbar\omega J_x\ , \tag{1}$$

where $H_{\rm intr}=H_{\rm sp}+H_p$ is the intrinsic Hamiltonian, including the axially deformed single-particle Hamiltonian $H_{\rm sp}$ (e.g., the Nilsson Hamiltonian) and the pairing interaction H_p. Although there exist some inherent defects (e.g., angular momentum nonconservation, etc.) the CSM has been proved to be very fruitful in the theoretical description on nuclear high-spin phenomena as well as the analysis of experimental data. For detailed reviews of the CSM, please see Refs. 13–15. The attractive features of the CSM (Ref. 15) are (a) that the collective and single-particle aspects of nuclear structure can be treated on the same footing and (b) that the calculation is simple for high spin as well as for low spin. Usually, the eigenvalue problem of the CSM is treated by the Hartree-Fock-Bogoliubov (HFB) approximation, i.e., the independent quasiparticle description. In view of the serious defects of the quasiparticle description of the nuclear pairing interaction[16] (e.g., the particle-number nonconservation, the excessive spurious states, the important blocking effects which cannot be taken into account properly, etc.), we prefer to adopt a particle-number-conserving (PNC) approach to treat the nuclear pairing Hamiltonian[17] and the low-lying eigenstates of the CSM Hamiltonian.[18]

In the previous paper[19] the K structure of the CSM wave function was investigated and it was shown that the accurate solution to the low-lying eigenstates of the CSM Hamiltonian can be obtained easily by the PNC approach with a many-particle configuration (MPC) truncation[20] plus K truncation.[19] Considering the angular momentum projection selection rule for the Coriolis interaction, $\Delta K=\pm 1$, such an approach is especially effective for treating the low-lying $K^\pi=0^+$ bands in the low-ω region. In this case, the number of K values involved is usually

very limited, i.e., only a few K values need to be considered. This means that the dimension of the MPC space, in which $H_{\rm CSM}$ is to be diagonalized to obtain the low-lying eigenstates, is greatly reduced. Therefore, the moments of inertia of the low-lying excited $K^\pi=0^+$ bands around the bandhead can be calculated much more easily.

It is well known[21] that the intruder high-j orbits play a decisive role in the analysis of the yrast spectra and the low-lying bands of deformed nuclei. In Sec. II we shall give an estimate of the moments of inertia of the low-lying $K^\pi=0^+$ bands in a single-j model ($j=\frac{13}{2}$ for neutron and $j=\frac{11}{2}$ for proton). In Sec. III, as an illustrative example, the moments of inertia of the low-lying $K^\pi=0^+$ bands well established in ^{168}Er are anlalyzed in some detail. A brief summary is given in Sec. IV.

II. ESTIMATE OF THE MOMENT OF INERTIA IN A SINGLE-j MODEL

In this section we shall give an estimate of the moments of inertia of the $K^\pi=0^+$ bands in a single-j model. When we investigate the effect of rotational motion on nuclear structure, particles in high-j orbits play a crucial role since the rotational perturbation is so strong in high-j orbits that even a small rotational motion can force the angular momentum of the particles to align along the rotational axis.[21] For example, the first backbending in rare-earth nuclei is often attributed to the alignment of a pair of neutrons occupying the intruder shell $i\frac{13}{2}$. Just as the intruder shells are essential for explaining the observed magic numbers in medium and heavy spherical nuclei, it is expected that in superdeformed high-spin states, the intruder shells also play an important role for nuclear structure.[22] Experimentally it was observed that the moment of inertia of an odd-A nucleus whose unpaired nucleon occupying the high-j intruder orbit is systematically much larger than the ground band moments of inertia of neighboring even-even nuclei. Some typical examples are shown in Table I. For example, the moment of inertia of the ground band ([633]7/2$^+$) of ^{169}Yb is $2\mathcal{I}/\hbar^2=123.7$ MeV^{-1}, which is much larger than that in ^{168}Yb ($2\mathcal{I}/\hbar^2=68.39$ MeV^{-1}) and ^{170}Yb ($2\mathcal{I}/\hbar^2=71.21$ MeV^{-1}). Therefore, it is expected that the nuclear moment of inertia comes mainly from the contribution of the nucleons in the intruder high-j orbits. This is partly due to the much stronger Coriolis response of the nucleons in the high-j orbits and partly due to the important blocking effects.

The single-particle energy is expressed as[23,24]

$$\varepsilon_{|\Omega|}=\kappa\frac{3\Omega^2-j(j+1)}{j(j+1)}+e_0,\quad |\Omega|=\tfrac{1}{2},\tfrac{3}{2},\ldots,j\ .$$

By choosing $e_0=6.655\hbar\omega_0$ and $\kappa=0.392\hbar\omega_0$ ($\sim$2.5–3.0 MeV), $j=\frac{13}{2}$, we may reproduce the Nilsson neutron levels of even parity at the deformation $\varepsilon_2=0.27$ and $\varepsilon_4=0.02$, corresponding roughly to the ground-state deformation of ^{168}Er, within 0.1%. This gives a certain realism to the single-j model. Furthermore, since the wave functions of high-j orbits are especially simple, the structure of the rotational perturbation can be analyzed and understood in a relatively straightforward way.[21] In the single-j model, the number of particles $N\le 2j+1$. The dimensions of the $r=+1$ MPC space ($E_c=\infty$) with and without K truncation for various N systems are shown in Table II. It is seen that the reduction in dimension achieved by K truncation is quite considerable. Nevertheless, the calculated results obtained by using K truncation faithfully reproduce the corresponding results obtained without K truncation.

When $\omega=0$, the magnitude of the nuclear angular momentum projection on the symmetry axis, K, is a good quantum number. When the Coriolis interaction is switched on ($\omega\neq 0$), the components of different K values will be mixed with each other, but in the low-ω region only one K value is dominant for a band and hence can be used to label the band approximately. The calculation shows that around the bandhead (low-ω region) the weights of the $K>2$ configurations in the $K^\pi=0^+$ bands are extremely small and can be neglected completely. For example, the calculation in the single-j model ($j=\frac{13}{2}$) shows that the K structures of the 0_1^+, 0_2^+, and 0_3^+ bands for the $N=8$ system at $\omega/\kappa=0.01$ ($\hbar\omega\sim 25$ keV) are as follows.

TABLE I. Even-odd difference of moment of inertia. Column 2 lists the moments of inertia of odd-A nuclei whose unpaired particle occupies the high-j orbit [633]7/2. Columns 3 and 4 give the ground band moments of inertia of neighboring even-even nuclei. Column 5 is the ratio $2\mathcal{I}(A)/[\mathcal{I}(A-1)+\mathcal{I}(A+1)]$.

Nuclei	$\frac{2\mathcal{I}(A)}{\hbar^2}$ (MeV^{-1})	$\frac{2\mathcal{I}(A-1)}{\hbar^2}$ (MeV^{-1})	$\frac{2\mathcal{I}(A+1)}{\hbar^2}$ (MeV^{-1})	$\frac{2\mathcal{I}(A)}{\mathcal{I}(A-1)+\mathcal{I}(A+1)}$
^{165}Dy	107.5	81.75	78.35	1.34
^{167}Er	112.4	74.47	75.18	1.50
^{169}Er	122.3	75.18	76.36	1.61
^{169}Yb	123.7	68.39	71.21	1.77
^{171}Yb	122.1	71.21	76.19	1.66
^{173}Yb	145.6	76.19	78.45	1.88
^{171}Hf	136.8	59.52	62.99	2.23
^{173}Hf	143.4	62.99	65.93	2.22
^{175}Hf	156.5	65.93	67.91	2.34
Average	130	72		1.80

TABLE II. Reduction in dimension of the MPC space, achieved by the K truncation. N is the particle number.

	$D(N)$			
	$j=\frac{13}{2}$		$j=\frac{11}{2}$	
N	No K truncation	$K\le 2$	No K truncation	$K\le 2$
2	49	19	36	16
4	511	144	255	86
6	1295	344	472	149
8	1295	344	255	86
10	511	144	36	16
12	49	19	1	1

K	0_1^+	0_2^+	0_3^+
0	0.9959	0.9803	0.9599
1	0.0041	0.0196	0.0397
2	0.0000	0.0001	0.0003

In Table III are presented the amplitudes of the configurations with weight $\geq 10^{-4}$ in the $K^\pi=0_1^+$ and 0_2^+ states for the $N=8$ system at $\omega/\kappa=0.01$. In the yrast band there is only one $K=1$ configuration with weight $>10^{-4}$—the lowest seniority $v=2$ configuration $123(\bar{4}5)$, in which the three pairs of particles occupy the single-particle levels 1 ($|\Omega|=\frac{1}{2}$), 2 ($|\Omega|=\frac{3}{2}$), and 3 ($|\Omega|=\frac{5}{2}$) and the two unpaired particles block the single-particle states 4 ($\Omega=\frac{7}{2}$) and 5 ($\Omega=\frac{9}{2}$) with resultant $K=1$. (Hereinafter an abbreviated notation of configuration is adopted, see Ref. 19 for details.) In the $K^\pi=0_2^+$ band the $K=1$ configurations with weight $>10^{-4}$ are the $v=2$ configurations $123(\bar{4}5)$, $125(\bar{3}4)$, $126(\bar{3}4)$, $123(\bar{5}6)$, $124(\bar{5}6)$, and $145(\bar{2}3)$. The components of the other $K\geq 1$ configurations are extremely small although these configurations are very numerous. Therefore, the solutions to the $K^\pi=0^+$ bands in the low-ω region thus obtained are very accurate and the information extracted from them is quite reliable.

Obviously, the angular momentum alignment along the rotating x axis, $\langle J_x\rangle$, and hence the moment of inertia, $\mathcal{J}=\langle J_x\rangle/\omega$, is strictly zero in an eigenstate of J_z for an

TABLE III. The non-negligible configurations (weight $>10^{-4}$) in the 0_1^+ and 0_2^+ bands of the eight-particle system at $\omega/\kappa=0.01$ ($\hbar\omega\sim 25$ keV). Columns 1, 2, and 3 list the configurations, the corresponding K values, and configuration energies, respectively. Columns 4 and 5 give the amplitudes of the non-negligible configurations in the 0_1^+ and 0_2^+ bands, respectively. The main configurations (weight $>10^{-2}$) are specified by *. In column 1, 1234 means a $v=0$ configuration in which the single-particle levels 1, 2, 3, and 4 are each occupied by one pair of particles; $123(\bar{4}5)$ represents a pair-broken configuration in which the three pairs of particles occupy the single-particle levels 1, 2, and 3, and the unpaired particles block the single-particle states 4 and 5 with resultant $K=\Omega_5-\Omega_4$, etc. The figures 1, 2, . . . , 7 stand for the single-particle levels as follows (see Fig. 1): 1≡[660]1/2, 2≡[651]3/2, 3≡[642]5/2, 4≡[633]7/2, 5≡[624]9/2, 6≡[615]11/2, 7≡[606]13/2.

Configurations	K	Configuration energies (in units of κ)	Amplitudes in 0_1^+ band	Amplitudes in 0_2^+ band
1234	0	0.0000	0.9470*	−0.2530*
1235	0	0.9846	0.1989*	0.9059*
1236	0	2.1254	0.0919	0.1052*
1237	0	3.6923	0.0549	0.0480
1245	0	1.7231	0.1211*	0.1963*
1246	0	2.9538	0.0663	0.0131
1247	0	4.4308	0.0428	
1256	0	3.9385	0.0205	0.0699
1257	0	5.4154	0.0131	0.0442
1345	0	2.2154	0.0959	0.1249*
1346	0	3.4462	0.0561	
1347	0	4.9231	0.0376	
1356	0	4.4308	0.0171	0.0569
1357	0	5.9077	0.0112	0.0373
1456	0	5.1692	0.0116	0.0180
1457	0	6.6462		0.0118
2345	0	2.4615	0.0868	0.1057*
2346	0	3.6923	0.0521	
2347	0	5.1692	0.0355	
2356	0	4.6769	0.0157	0.0524
2357	0	6.1538	0.0104	0.0349
2456	0	5.4154	0.0107	0.0162
2457	0	6.8923		0.0107
3456	0	5.9077		0.0119
$123(\bar{4}5)$	1	0.4923	−0.0619	0.0962
$125(\bar{3}4)$	1	1.3538		−0.0868
$126(\bar{3}4)$	1	2.5846		−0.0113
$123(\bar{5}6)$	1	1.6000		−0.0452
$124(\bar{5}6)$	1	2.3385		−0.0103
$145(\bar{2}3)$	1	1.9692		−0.0133

even-N system. When the Coriolis interaction is switched on ($\omega \neq 0$) K no longer remains a good quantum number and the $K>0$ configurations, first of all the $K=1$ configurations, are gradually mixed into the $K^{\pi}=0^{+}$ band. The moment of inertia of each band around the bandhead depends sensitively on the amplitudes (magnitude and phase) of these $K=1$ configurations.

The calculated moments of inertia of three low-lying $K^{\pi}=0^{+}$ bands in the single-j model are shown in Figs. 1 and 2 along with the single-particle level schemes. Figure 1 is for the $i13/2$ neutrons and Fig. 2 for the $h11/2$ protons. The Fermi surface shifts upwards with increasing N, the number of particles in high-j orbits. From Figs. 1 and 2 the following features about the moments of inertia can be drawn.

(1) In the single-j model, the moment of inertia of the lowest excited $K^{\pi}=0^{+}$ band is systematically larger than that of the ground band, i.e., $\mathcal{I}(0_2^+)>\mathcal{I}(0_1^+)$, which can be understood qualitatively from the dense distribution (see Figs. 1 and 2) of the excited states (above the energy gap), which are strongly coupled with each other by the Coriolis interaction. Quantitatively, the result $\mathcal{I}(0_2^+)>\mathcal{I}(0_1^+)$ can be accounted for from the individual contributions to the moments of inertia of 0_1^+ and 0_2^+ bands. As an example, the result for an eight-particle system in the single-j model ($j=\frac{13}{2}$) is listed in Table IV. It is seen that the main contributions to the angular momentum alignment $\langle J_x \rangle$ for the 0_1^+ band at $\omega/\kappa=0.01$ are

$$2\times 0.9470\times(-0.0619)\times\langle 1234|J_x|123(\bar{4}5)\rangle=0.4762\ ,$$

$$2\times 0.1989\times(-0.0619)\times\langle 1235|J_x|123(\bar{4}5)\rangle=0.1000\ ,$$

which correspond to a particle jumping from the $[633]7/2^{+}$ state to the $[624]9/2^{+}$ state, then a $K=1$ configuration formed. The resultant $\langle J_x \rangle=0.6646$ (at $\omega/\kappa=0.01$) means that, for the whole system, the angular momentum alignment along the rotating x axis has appeared. The individual contributions to the 0_2^+ band moment of inertia are more complicated as shown in Table IV. Because a number of configurations are responsible for the $\langle J_x \rangle$, though some main contributions cancel each other, the resultant angular momentum alignment is still larger ($\sim 17\%$) than the 0_1^+ band. Similarly, we have $\mathcal{I}(0_3^+)>\mathcal{I}(0_1^+)$.

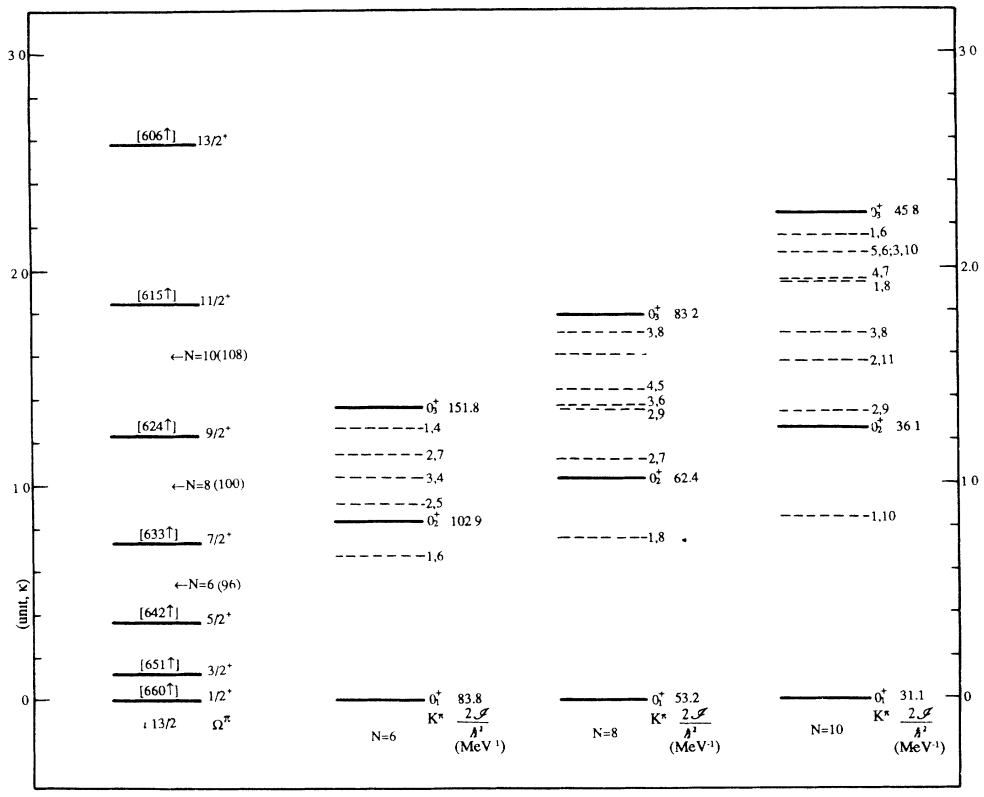

FIG. 1. The low-lying eigenspectra (at $\omega=0$) of the single-j ($j=\frac{13}{2}$) cranked-shell-model Hamiltonian for $N=6$, 8, and 10 particle systems. The pair-excitational states ($K^{\pi}=0^{+}$) are indicated by the bold lines and to the right side of each bold line are shown the corresponding moments of inertia ($2\mathcal{I}/\hbar^2$). The dashed lines represent the pair-broken states, $K=|\Omega_1 \pm \Omega_2|$, where the unpaired particles occupy the single-particle levels Ω_1 and Ω_2 separately. The left part of Fig. 1 is the single-particle levels scheme ($i13/2$) where the conventional Nilsson notation $[Nn_z\Lambda]\Omega\pi$ is used. The arrows indicate the position of Fermi surface for various N-particle systems and the number of neutrons in realistic rare-earth nuclei corresponding to each case is indicated in the bracket.

TABLE IV. Main contributions (larger than 0.005) to $\langle J_x \rangle$ of the 0_1^+ and 0_2^+ bands for an eight-particle system in single-j model ($j=\frac{13}{2}$) at $\omega/\kappa=0.01$. The pair of configurations responsible for $\langle J_x \rangle$ are listed in columns 1 and 2 and the corresponding single-particle transition is given in column 3. The contributions to $\langle J_x \rangle$ of the 0_1^+ and 0_2^+ bands are given in columns 4 and 5, respectively.

Configurations responsible for $\langle J_x \rangle$	Single-particle transitions	Contributions to 0_1^+ band	Contributions to 0_2^+ band
1234, 123($\bar{4}$5)	[633]7/2↔[624]9/2	0.4762	0.1978
1235, 123($\bar{4}$5)	[633]7/2↔[624]9/2	0.1000	−0.7082
1235, 125($\bar{3}$4)	[642]5/2↔[633]7/2	0.0166	0.7036
1236, 126($\bar{3}$4)	[642]5/2↔[633]7/2		0.0106
1245, 125($\bar{3}$4)	[642]5/2↔[633]7/2	0.0100	0.1524
1235, 123($\bar{5}$6)	[624]9/2↔[615]11/2	0.0082	0.2840
1236, 123($\bar{5}$6)	[624]9/2↔[615]11/2		0.0330
1245, 124($\bar{5}$6)	[624]9/2↔[615]11/2		0.0140
1345, 134($\bar{5}$6)	[624]9/2↔[615]11/2		0.0058
1245, 145($\bar{2}$3)	[651]3/2↔[642]5/2	0.0056	0.0248
1345, 145($\bar{2}$3)	[651]3/2↔[642]5/2		0.0158
1345, 345($\bar{1}$2)	[660]1/2↔[651]3/2		0.0092
2345, 345($\bar{1}$2)	[660]1/2↔[651]3/2		0.0078

(2) When the Fermi surface lies near the bottom of the high-j shell the ground band moment of inertia is larger because of the strong Coriolis response of the nucleons in the high-j low-Ω orbits; i.e., the higher the Fermi surface, the smaller the ground band moment of inertia.

(3) The contribution to the moment of inertia from the high-j shell depends sensitively on the j value. For example, the moment of inertia of the 0_1^+ band for the $N=6$ system in the $j=\frac{13}{2}$ shell is about twice as large as that in the $j=\frac{11}{2}$ shell.

Now let us assume that there are eight neutrons in the $i13/2$ shell and eight protons in the $h11/2$ shell, which may be served as a simulation of the high-j shells in $^{168}_{68}\mathrm{Er}_{100}$ (see Fig. 3). From Figs. 1 and 2 we obtain the ground band moment of inertia

$$2\mathcal{I}/\hbar^2=2(\mathcal{I}_n+\mathcal{I}_p)/\hbar^2\approx 77\ \mathrm{MeV}^{-1}\ ,$$

which is very close to the observed ground band moment of inertia of ^{168}Er (75.2 MeV^{-1}). This coincidence may be more or less accidental, nevertheless, we believe that the nucleons in the high-j intruder orbits do play an essential role in the nuclear moment of inertia and some characteristic features of the moments of inertia may be manifested in the single-j model. Calculations by using a more realistic single-particle level scheme (see Sec. III) indeed confirm such an expectation.

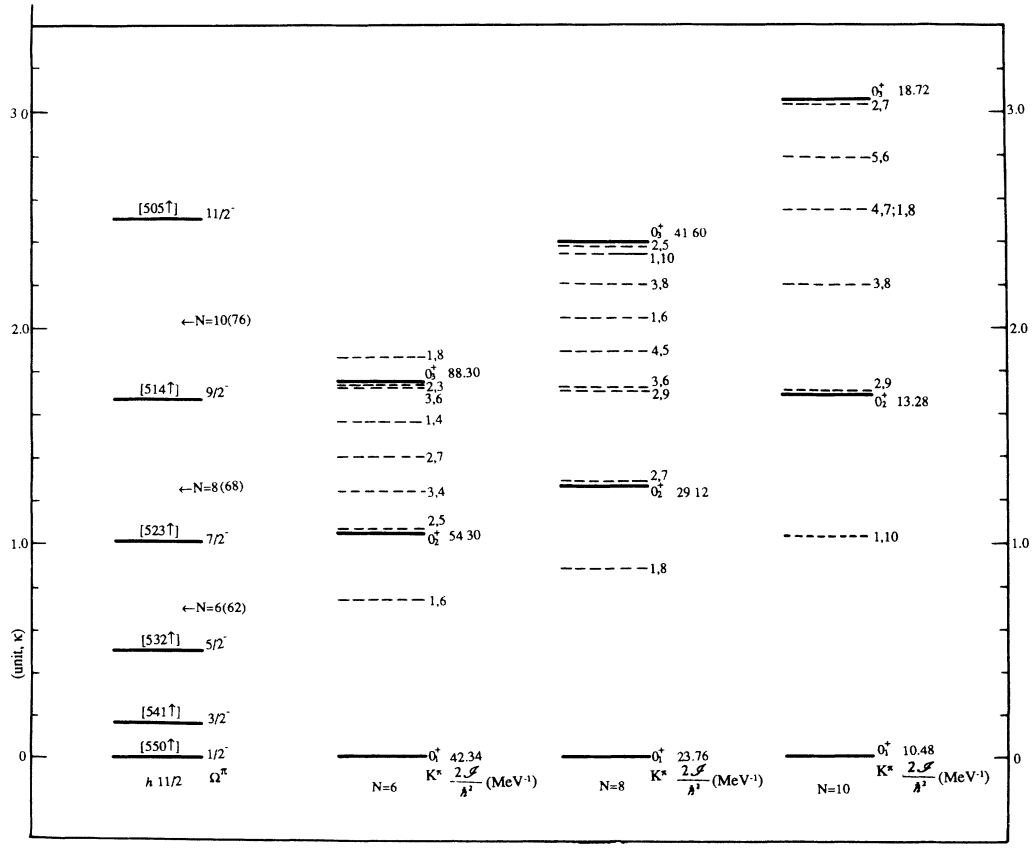

FIG. 2. The same as Fig. 1 but for $j=\frac{11}{2}$.

III. MOMENTS OF INERTIA OF THE $K^{\pi}=0^{+}$ BANDS IN ^{168}Er

A recent investigation of the ^{167}Er$(n,\gamma)^{168}$Er reaction led to the establishment of a level scheme for ^{168}Er, which is believed to be the most detailed and complete level scheme now available for an even-even deformed nucleus.[5-8] The overall level scheme comprising 36 rotational bands is known to be complete for levels with spin $I<6$ and excited energy $E_x<2$ MeV. Among them, four $K^{\pi}=0^{+}$ bands (bandhead <2 MeV) have been well established (see Fig. 5). In this section we shall calculate the moments of inertia of the low-lying $K^{\pi}=0^{+}$ bands in ^{168}Er in the framework of the CSM by using the particle-number-conserving approach. The accurate solutions to the low-lying eigenstates are obtained by diagonalizing $H_{\rm CSM}$ in a sufficiently large truncated MPC space.

It should be emphasized that in the calculation *no free parameter* is involved. The Nilsson level scheme for ^{168}Er is shown in Fig. 3. The single-particle potential parameters involved are chosen according to the Lund systematics,[25,26] i.e.,

$$\varepsilon_2=0.273\ ,$$

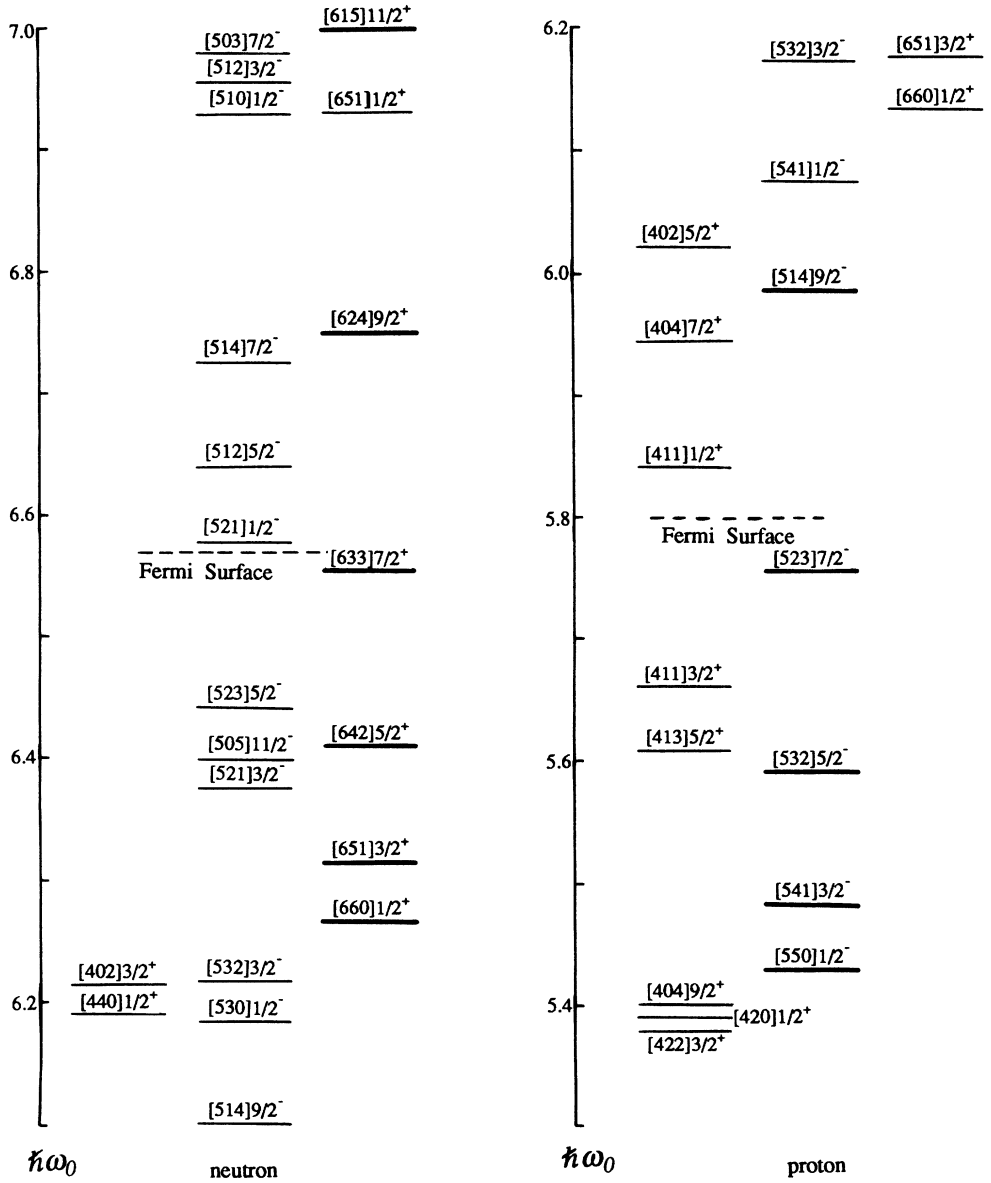

FIG. 3. The Nilsson level scheme around the Fermi surface in ^{168}Er (Lund systematics, see text).

$$\varepsilon_5=0.023\ ,$$

$$\mu_n=0.624-1.234\times A\times 10^{-3}\ ,$$

$$\kappa_n=0.0641-2.6\times A\times 10^{-6}\ ,$$

$$\mu_p=0.493+0.649\times A\times 10^{-3}\ ,$$

$$\kappa_p=0.0766-77.9\times A\times 10^{-6}\ ,$$

and the harmonic-oscillator strength parameters are

$$\hbar\omega_{0n}=41\,A^{-1/3}\left[1+\frac{N-Z}{3A}\right]\simeq 7.902\ \text{MeV}\ ,$$

$$\hbar\omega_{0p}=41\,A^{-1/3}\left[1-\frac{N-Z}{3A}\right]\simeq 6.959\ \text{MeV}\ .$$

The pairing interaction strengths G_n and G_p are determined by the even-odd mass differences[17]

$$P_n=\tfrac{1}{2}[B(^{168}\text{Er})+B(^{170}\text{Er})]-B(^{169}\text{Er})$$
$$=0.6280\ \text{MeV}\ ,$$

$$P_p=\tfrac{1}{2}[B(^{168}\text{Er}+B(^{170}\text{Yb})]-B(^{169}\text{Tm})$$
$$=0.6040\ \text{MeV}\ ,$$

where the B's are the nuclear binding energies taken from the 1983 Atomic Mass Table.[27] By choosing a sufficiently large MPC truncation energy, $E_c=0.5\hbar\omega_0$ (about 20 single-particle levels around the Fermi surface being involved, see Fig. 3), we get

$$G_n\approx 0.040\,60\hbar\omega_{0n}\ ,$$

$$G_p\approx 0.056\,88\hbar\omega_{0p}\ .$$

Because we are interested in the properties of low-lying $K^{\pi}=0^{+}$ bands around the bandhead it is very convenient to adopt the K truncation, namely, H_{CSM} is diagonalized in the MPC subspace with $K\le 2$.

The calculated low-lying $K^{\pi}=0^{+}$ bands (at $\omega=0$) and their moments of inertia are shown in Fig. 4. The left portion of Fig. 4 is for the neutron system and the right portion for the proton system. Below $E_x\le 2.6$ MeV there are three neutron pair-excitational states (the ground state $n0_1^+$ with $2\mathcal{J}_n/\hbar^2=51.6\ \text{MeV}^{-1}$, $n0_2^+$ at 1359 keV with $2\mathcal{J}_n/\hbar^2=80\ \text{MeV}^{-1}$, and $n0_3^+$ at 2118 keV with $2\mathcal{J}_n/\hbar^2=63.7\ \text{MeV}^{-1}$) and two proton pair-excitational states (the ground state $p0_1^+$ with $2\mathcal{J}_p/\hbar^2=26.5\ \text{MeV}^{-1}$ and $p0_2^+$ at 1637 keV with $2\mathcal{J}_p/\hbar^2=33.9\ \text{MeV}^{-1}$). Therefore, the moment of inertia of the ground band in ^{168}Er is

$$2\mathcal{J}_0/\hbar^2=(51.6+26.5)\ \text{MeV}^{-1}=78.1\ \text{MeV}^{-1}$$

which is very close to the observed value 75.2 MeV^{-1} (see Fig. 5). Considering the fact that no free parameter is involved in the calculation, the agreement between the calculated and the observed ground band moment of inertia is encouraging. It is seen that the major contribution to the moment of inertia ($\sim\frac{2}{3}$) comes from the neutron system and the remaining part ($\sim\frac{1}{3}$) comes from the proton system. It is worthwhile to mention that, like the results in Ref. 12, it does not seem necessary to have an extra contribution from an inert core, $\mathcal{J}_c(=60/\kappa\approx 24\ \text{MeV}^{-1}$, cf. Refs. 23 and 24), to account for the observed nuclear moment of inertia.

It is interesting to note that the $n0_2^+$ band moment of inertia is much larger than that of the $n0_1^+$ band. This result can be easily understood from the structure of wave function around the bandhead (see Table V). From Table VI it is seen that one of the most important contributions to the angular momentum alignment $\langle J_x\rangle$ at $\omega/\omega_{0n}\sim 0.05$ ($\hbar\omega\sim 40$ keV) is

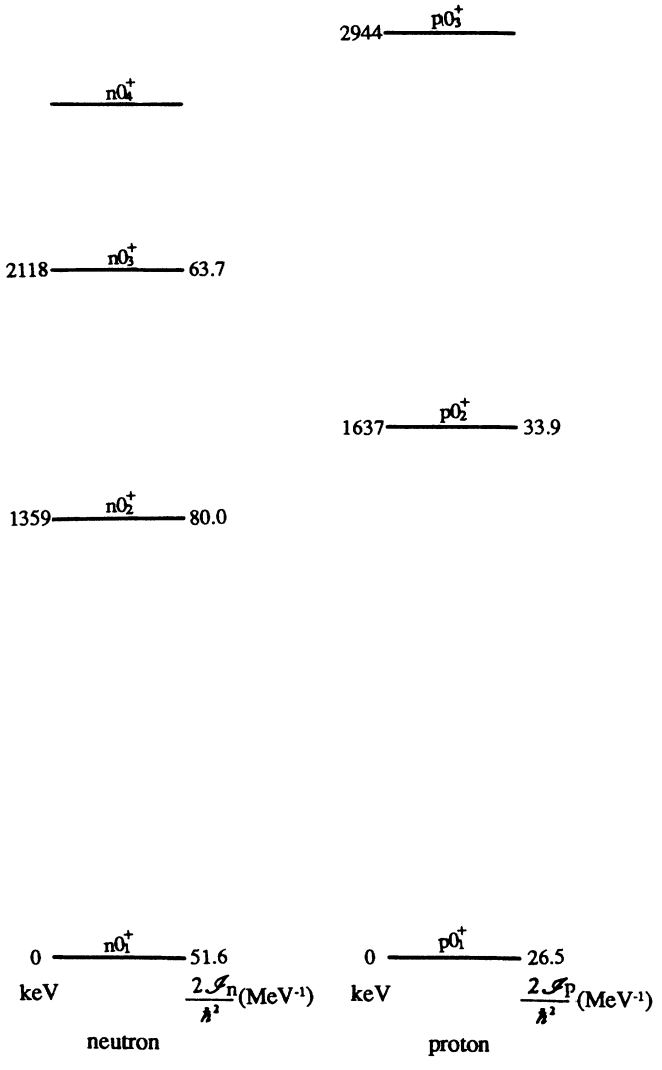

FIG. 4. The calculated low-lying ($E_x<2$ MeV) neutron and proton pair-excitational $K^{\pi}=0^{+}$ bands at $\omega=0$ (i.e., bandheads) in ^{168}Er. The corresponding moments of inertia are also given to the right of each bandhead.

$$2\times\sqrt{2}\times0.5135\times0.0461\times\langle[642]5/2|J_x|[633]7/2\rangle = 0.2044$$

for the 0_1^+ band

$$2\times\sqrt{2}\times0.7463\times0.1036\langle[642]5/2|J_x|[633]7/2\rangle = 0.6676$$

for the 0_2^+ band which leads to a much larger moment of inertia for the 0_2^+ band than for the 0_1^+ band. In fact, the occupation probability of the first Nilsson level immediately below the Fermi surface ([633]7/2, see Fig. 3) in the 0_2^+ band is smaller that in the 0_1^+ band, hence, the neutron pair in the lower high-j orbit [642]5/2 has a larger probability to be excited to the relatively vacant level [633]7/2 orbit and results in a larger contribution to $\langle J_x\rangle$ for the 0_2^+ band. Another important contribution to $\langle J_x\rangle$ is

$$2\times\sqrt{2}\times0.6846\times0.0467\times\langle[633]7/2|J_x|[624]9/2\rangle = 0.2534$$

for the 0_1^+ band

$$2\times\sqrt{2}\times0.6229\times0.0660\times\langle[633]7/2|J_x|[624]9/2\rangle = 0.3262$$

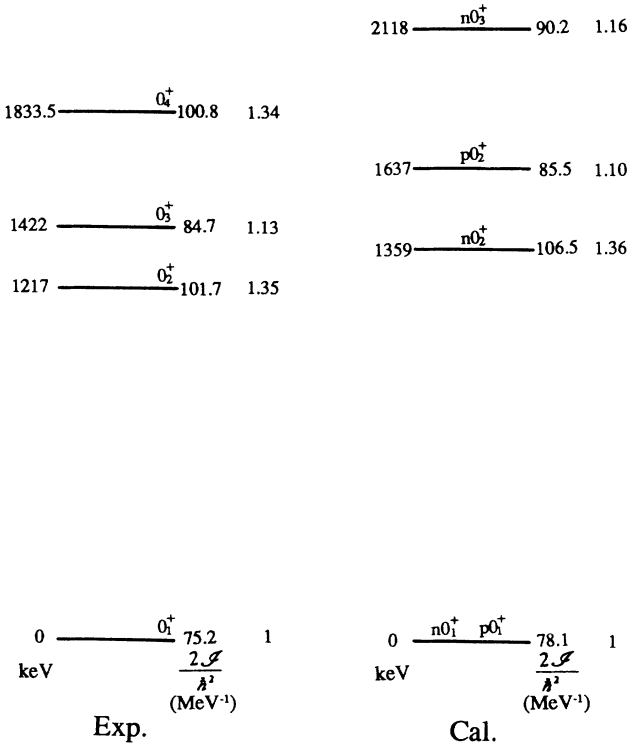

FIG. 5. The moments of inertia of the low-lying $K^\pi=0^+$ bands in ^{168}Er. The left portion shows the observed results and the right portion gives the calculated results for the ground band and three lowest pair-excitational bands.

for the 0_2^+ band which also leads to a larger moment of inertia for the 0_2^+ band compared with that for the 0_1^+ band. A similar situation occurs in some other contributions.

It is seen from the discussion above that a satisfactory explanation of the moments of inertia in ^{168}Er can be obtained in the PNC treatment of the usual CSM Hamiltonian,[14,15] in which only a monopole pairing interaction is included. The great success of such a simple CSM (Ref. 14) in the description on nuclear high-spin phenomena has been generally recognized in recent years. The reason is that, just as pointed out by Hamamoto and Mottelson,[21] the major part of the two-body long-range interactions in the spherical shell model could be absorbed into the average one-body deformed field and, thus, only a week residual two-body long-range interaction remains to be taken into account. This statement is supported by the well-known success of the Nilsson model[26] in providing the basis for the classification of the extensive body of data on odd-A deformed nuclei. In addition, the sys-

TABLE V. The same as Table III but for the neutron configurations in ^{168}Er at $\omega/\omega_{0n}=0.05$. The figures and alphabets in column 1 stand for the Nilsson levels as follows:

1≡[514]9/2,	2≡[530]1/2,	3≡[400]1/2,	4≡[402]3/2,
5≡[532]3/2,	6≡[660]1/2,	7≡[651]3/2,	8≡[521]3/2,
9≡[505]11/2,	a≡[642]5/2,	b≡[523]5/2,	c≡[633]7/2,
d≡[521]1/2,	e≡[512]5/2,	f≡[514]7/2,	g≡[624]9/2,
h≡[510]1/2,	i≡[651]1/2,	j≡[512]3/2.	

Configurations	K	Configuration energies (in units of $\hbar\omega_0$)	Amplitudes in 0_1^+ band	Amplitudes in 0_2^+ band
123456789*abc*	0	0.0000	0.6846*	−0.6229*
123456789*abd*	0	0.0427	0.5135*	0.7463*
123456789*abe*	0	0.1682	0.2727*	0.0585
123456789*abf*	0	0.3398	0.1415*	0.0293
123456789*abg*	0	0.3882	0.1303*	0.0215
123456789*acd*	0	0.2693	0.1927*	0.0446
123456789*ace*	0	0.3948	0.1120*	−0.0643
123456789*ade*	0	0.4375	0.0847	0.0905
123456789*bcd*	0	0.3303	0.1688*	0.0432
123456789*bce*	0	0.4558	0.0994	−0.0559
123456789*bde*	0	0.4985	0.0746	0.0798
12345678*abcd*	0	0.3562	0.1515*	0.0233
12345678*abce*	0	0.4817	0.0889	−0.0621
12345679*abcd*	0	0.4021	0.1328*	0.0270
123456789*bd*($\bar{a}c$)	1	0.1865	−0.0461	−0.1036*
123456789*be*($\bar{a}c$)	1	0.3120	−0.0217	−0.0157
123456789*bf*($\bar{a}c$)	1	0.4836		−0.0115
123456789*ab*($\bar{c}g$)	1	0.1941	−0.0467	0.0660
12345679*abc*($\bar{8}e$)	1	0.2638	0.0224	−0.0272
12345679*abd*($\bar{8}e$)	1	0.3065	0.0162	0.0290
123456789*ac*($\bar{b}f$)	1	0.2832	−0.0223	0.0253
123456789*ad*($\bar{b}f$)	1	0.3259	−0.0163	−0.0279
12346789*abc*($\bar{5}d$)	1	0.3586		0.0129
13456789*abc*(2*d*)	1	0.3909		−0.0118
123456789*ab*(*dh*)	1	0.3934		−0.0178
123456789*ab*($\bar{d}j$)	1	0.4202		−0.0170

tematical behavior of the ground band moments of inertia in the rare-earth nuclei was reproduced well in the work by Nilssson *et al.*[12]

Of course, the usual CSM is too simple to account for all the detailed behavior of nuclear moment of inertia. For a more satisfactory description of nuclear moment of inertia, it seems necessary to include the other residual interactions, such as the quadrupole-quadrupole interaction, the spin-dependent interaction, and the higher multipole pairing interaction, etc. The PNC formalism for treating the pairing plus quadrupole-quadrupole interaction has been given in Ref. 28. The calculation shows that the quadrupole-quadrupole interaction would be important for collectively excited bands, e.g., the γ-vibrational bands. However, its influence on the moments of inertia of the $K^{\pi}=0^{+}$ bands with less collective character is not expected to be large.

IV. SUMMARY

The nuclear moment of inertia is one of the most important properties characterizing a rotational band. The CSM of Inglis[9] provides a basis for interpreting the moment of inertia. By using the quasiparticle formalism and the second-order perturbation theory, Nilsson *et al.*[12] succeeded in explaining the importnat fact that the observed ground band moments of inertia of even-even deformed nuclei are about $\frac{1}{3}$ to $\frac{1}{2}$ of the rigid-body value. In the present paper the moments of inertia of the $K^{\pi}=0^{+}$ bands in well-deformed nuclei are calculated in the framework of the CSM by using a PNC approach, associated with a MPC truncation pluse a K truncation. In virtue of the angular momentum projection selection rule for the Coriolis interaction, $\Delta K=\pm 1$, this approach turns out to be very effective for calculating the nuclear moment of inertia.

The calculation shows that the intruder high-j orbits play a decisive role in nuclear moment of inertia. In fact, the vast majority of nuclear moment of inertia comes from the contribution of nucleons in the high-j orbits and the calculation in a single-j model does reproduce the characteristic features of nuclear moment of inertia, e.g., the ground band moment of inertia, the markedly different moments of inertia of the low-lying excited $K^{\pi}=0^{+}$ bands from the ground band value, etc. If we assume that the low-lying $K^{\pi}=0^{+}$ bands established in ^{168}Er are low-lying neutron pair-excitational or proton excitational states, or a certain superposition of them, the agreement between the calculated and the observed moments of inertia is very satisfactory, though no free parameter appears in the calculation. The calculation shows that the moment of inertia depends sensitively on the properties and the distribution of the single-particle levels around the Fermi surface, especially the position of the intruder high-j orbits. Thus, the investigation in nuclear moment of inertia may provide us with valuable in-

TABLE VI. The same as Table IV but for the neutron configurations in ^{168}Er at $\omega/\omega_{0n}=0.05$ (contributions larger than 0.01).

Configurations responsible for $\langle J_x \rangle$	Single-particle transitions	Contributions to 0_1^+ band	Contributions to 0_2^+ band
123456789*abc*, 123456789*ab*($\bar{c}g$)	[633]7/2↔[624]9/2	0.2534	0.3262
123456789*abg*, 123456789*ab*($\bar{c}g$)	[633]7/2↔[624]9/2	0.0482	−0.0112
123456789*acd*, 123456789*ad*($\bar{c}g$)	[633]7/2↔[624]9/2	0.0140	
123456789*abd*, 123456789*bd*($\bar{a}c$)	[642]5/2↔[633]7/2	0.2044	0.6676
123456789*abe*, 123456789*be*($\bar{a}c$)	[642]5/2↔[633]7/2	0.0512	
123456789*abf*, 123456789*bf*($\bar{a}c$)	[642]5/2↔[633]7/2	0.0110	
123456789*bcd*, 123456789*bd*($\bar{a}c$)	[642]5/2↔[633]7/2	0.0672	0.0386
123456789*bce*, 123456789*be*($\bar{a}c$)	[642]5/2↔[633]7/2	0.0186	
123456789*bcd*, 12345689*bcd*($\bar{7}a$)	[651]3/2↔[642]5/2	0.0100	
123456789*abc*, 12345679*abc*($\bar{8}e$)	[521]3/2↔[512]5/2	0.0792	0.0874
123456789*abd*, 12345679*abd*($\bar{8}e$)	[521]3/2↔[512]5/2	0.0428	0.1118
123456789*abd*, 123456789*ab*($\bar{d}j$)	[521]1/2↔[512]3/2	0.0158	0.0472
123456789*abc*, 123456789*ac*($\bar{b}f$)	[523]5/2↔[514]7/2	0.0794	0.0818
123456789*abd*, 123456789*ad*($\bar{b}f$)	[523]5/2↔[514]7/2	0.0436	0.1082
123456789*abe*, 123456789*ae*($\bar{b}f$)	[523]5/2↔[514]7/2	0.0118	
123456789*abc*, 12346789*abc*($\bar{5}d$)	[532]3/2↔[521]1/2	0.0188	0.0232
123456789*abc*, 13456789*abc*(2*d*)	[530]1/2↔[521]1/2	0.0178	0.0214
123456789*abd*, 123456789*ab*(*dh*)	[510]1/2↔[521]1/2	0.0160	0.0490

formation on the single-particle level distribution around the Fermi surface.

In addition, the g factor, which is sensitive to the spin alignment, would provide a further test of the CSM wave function obtained using the PNC treatment. Recently, it was observed[29] that there exists a distinct difference between the behavior of g factors along the yrast line for ^{166}Er and that for ^{168}Er, i.e., the g factors in ^{166}Er decrease monotonically with increasing angular momentum I ($I=2-10$), while they remain nearly constant in ^{168}Er. A preliminary calculation shows that the g factors in ground bands of ^{166}Er and ^{168}Er and their distinct behavior can be reproduced well by using the particle-number-conserving CSM wave function.

[1]A. Bohr and B. R. Mottelson, *Nuclear Deformations,* Vol. II of Nuclear Structure (Benjamin, New York, 1975).

[2]A. Bohr and B. R. Mottelson, Phys. Scr. **25**, 28 (1982).

[3]R. F. Casten and D. D. Warner, Rev. Mod. Phys. **60**, 389 (1988).

[4]S. Kuyucak and I. Morrison, Phys. Rev. C **38**, 2482 (1988).

[5]W. F. Davidson, D. D. Warner, R. F. Casten, K. Schreckenbach, H. G. Börner, J. Simic, M. Stoianovic, M. Bogdanovic, S. Koicki, W. Gelletlyly, G. B. Orr, and M. L. Steltz, J. Phys. G **7**, 455 (1981); **7**, 843 (1981).

[6]W. F. Davidson, W. R. Dixon, and R. S. Storey, Can. J. Phys. **62**, 1538 (1984).

[7]D. D. Warner, R. F. Casten, and W. F. Davidson, Phys. Rev. C **24**, 1713 (1981).

[8]W. F. Davidson, W. R. Dixon, D. G. Burke, and J. A.Cizewski, Phys. Rev. **130B**, 161 (1983).

[9]D. R. Inglis, Phys. Rev. **95**, 1057 (1954).

[10]A. Bohr and B. R. Mottelson, Mat. Fys. Medd. Dan. Vid. Selsk. **30**, No. 1 (1955).

[11]S. T. Belyaev, Mat. Fys. Medd. Dan. Vid. Selsk. **31**, No. 11 (1959).

[12]S. G. Nilsson and O. Prior, Mat. Fys. Medd. Dan. Vid. Selsk. **32**, No. 16 (1960).

[13]A. Bohr and B. R. Mottelson, Jpn. J. Phys. Suppl. **44**, 152 (1978).

[14]R. Bengtsson and J. D. Garrett, Int. Rev. Nucl. Phys. **2**, 193 (1984).

[15]I. Hamamoto, in *Nuclear Structure,* edited by R. Broglia, G. B. Hagemann, and B. Herskind (Elsevier, New York, 1985), p. 129.

[16]For example, D. J. Rowe, *Nuclear Collective Motion* (Methuen, London, 1970), Chap. 11; L. F. Canto, P. Ring, and J. O. Rasmussen, Lawrence Berkeley Laboratory Report LBL-19519, 1985.

[17]J. Y. Zeng and T. S. Cheng, Nucl. Phys. **A405**, 1 (1983); J. Y. Zeng, T. S. Cheng, L. Cheng, and C. S. Wu, *ibid.* **A411**, 49 (1983); **A414**, 253 (1984); **A421**, 125 (1984).

[18]C. S. Wu and J. Y. Zeng, Phys. Rev. C **40**, 998 (1989).

[19]C. S. Wu and J. Y. Zeng, Phys. Rev. C **41**, 1822 (1990).

[20]C. S. Wu and J. Y. Zeng, Phys. Rev. C **39**, 666 (1989).

[21]I. Hamamoto and B. R. Mottelson, *Shell Model and High-Spin and Deformation,* Proceedings of the Symposium on the Occasion of the 40th Anniversary of Nuclear Shell Model, 1989 (Argonne National Laboratory, Argonne, 1989).

[22]T. Bengtsson, I. Ragnarsson, and S. Åberg, Phys. Lett. B **208**, 39 (1988).

[23]I. Hamamoto, Nucl. Phys. **A271**, 15 (1976).

[24]R. Bengtsson and B. H. Håkansson, Nucl. Phys. **A357**, 61 (1981).

[25]R. Bengtsson, S. Frauendorf, and F. R. May, At. Data Nucl. Data Tables **35**, 15 (1986).

[26]S. G. Nilsson, C. F. Tsang, A. Sobiczewski, Z. Szymanski, S. Wycech, C. Gustafson, I.-L. Lamm, P. Möller, and B. Nilsson, Nucl. Phys. **A131**, 1 (1969).

[27]A. H. Wapstra and G. Audi, Nucl. Phys. **A432**, 1 (1985).

[28]H. X. Huang, C. S. Wu, and J. Y. Zeng, High Energy Phys. Nucl. Phys. **13**, 193 (1989).

[29]C. E. Doran, H. H. Bolotin, A. E. Stuchbery, and A. P. Byrne, Z. Phys. A **325**, 285 (1986).